



On Practical Charge Injection at the Metal/Organic Semiconductor Interface

Akichika Kumatani^{1*}, Yun Li^{1†}, Peter Darmawan¹, Takeo Minari¹ & Kazuhito Tsukagoshi^{1,2}

¹WPI center for Materials Nanoarchitectonics (WPI-MANA), National Institute of Materials Science (NIMS), Tsukuba, Ibaraki 305-0044, Japan, ²CREST-JST, Kawaguchi, Saitama 332-0012, Japan.

SUBJECT AREAS:
MATERIALS CHEMISTRY
MATERIALS SCIENCE
ELECTRONIC DEVICES
APPLIED PHYSICS

Received
21 June 2012

Accepted
8 November 2012

Published
4 January 2013

Correspondence and requests for materials should be addressed to A.K. (KUMATANI@wpi-aimr.tohoku.ac.jp) or K.T. (TSUKAGOSHI.Kazuhiro@nims.go.jp)

* Current address: WPI-Advanced Institute for Materials Research (WPI-AIMR), Tohoku University, Sendai 980-8578, Japan.

† Current address: Key Laboratory of Photonic and Electronic Materials and School of Electronic Science and Engineering, Nanjing University, Nanjing 210093, People's Republic of China.

We have revealed practical charge injection at metal and organic semiconductor interface in organic field effect transistor configurations. We have developed a facile interface structure that consisted of double-layer electrodes in order to investigate the efficiency through contact metal dependence. The metal interlayer with few nanometers thickness between electrode and organic semiconductor drastically reduces the contact resistance at the interface. The improvement has clearly obtained when the interlayer is a metal with lower standard electrode potential of contact metals than large work function of the contact metals. The electrode potential also implies that the most dominant effect on the mechanism at the contact interface is induced by charge transfer. This mechanism represents a step forward towards understanding the fundamental physics of intrinsic charge injection in all organic devices.

The charge injection process at the metal and organic material interface has a large impact on the electrical properties of organic semiconductor devices, and is sometimes even more dominant than charge transport within the organic semiconductor. The charge injection barrier at the contact interface between a metal and an organic material is commonly described by the mechanism of metal to semiconductor contact¹. This provides the plausible explanation that a potential barrier is caused by the energy difference between the Fermi level of the metal and the energy band of the organic material². Therefore, the use of metals with sufficiently large work functions (W_F) is commonly considered to be the most important factor in controlling the potential barrier for charge injection. For the energy level alignment at the interface of the practical devices, natural oxidation at the metal surface under an ambient atmosphere is also important factor to be carefully considered. The natural oxidation of the metal is quite common as unavoidable a redox reaction in the practical device fabrication. The natural oxidation is a redox reaction between the metal and oxygen, so the reaction depends upon the standard electrode potential (E_p) of the metal³. Here, we report a significant effect of E_p of the contact metal on the organic semiconductor interface in organic devices, particularly the influence of natural oxidation of the contact metal. By fabrication of organic field-effect transistors (OFETs) having double-layer electrodes in an inert atmosphere, we have observed that the contact metal is spontaneously oxidized at the metal/organic interface under an ambient atmosphere, and that the formation of an oxide film strongly affects the charge injection efficiency of the organic devices. It is also found that, due to the formation of an oxide film at the contact interface, E_p is the most dominant factor influencing charge injection, rather than the W_F of the metal, once the devices were exposed to air. This phenomenon implies that even insulating oxide can be applicable for rectifying charge injection, which we have proven using silicon dioxide and aluminum oxide with low standard electrode potential. All organic devices with metal contacts is at risk of natural oxidation in an ambient atmosphere, so this discovered mechanism provides critical insight into the control of metal/organic interfaces in the practical application of plastic electronics.

Results

Here, in this experiment, we have characterized current injection resistance from metallic contact to organic semiconductor thin films to understand practical charge injection in OFETs. The current injection resistance is compared using double-layer electrodes with various thin metallic film covered by thick Au-film. We fabricated OFETs with double-layer source/drain electrodes consisting of a current providing layer and a charge injection interlayer, as shown in Fig. 1a. Pentacene, a common *p*-type organic semiconductor, was used as an active material. A thin layer of various metals with few nanometer thickness (2 nm) was inserted into the interface as a charge injection interlayer, allowing the direct and systematic investigation of the contact metal dependency. The contact resistance can be evaluated at the contact interface by using OFETs with double-layered electrodes. If the electrodes are designed with only a single-layer, the internal resistance depends upon only the metal itself (Au:

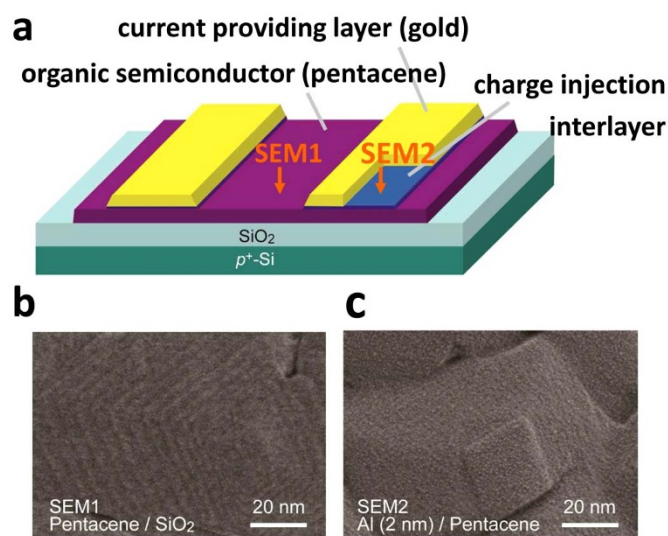


Figure 1 | (a) Schematic diagram of fabricated OFETs having double-layered electrode. The channel length varied from 20 to 140 μm with the interval of 20 μm was used for TLM analysis. SEM images (low acceleration voltage = 50 V) show the pentacene surface before (b) and after (c) charge injection interlayer was deposited on the pentacene with aluminium of 2 nm thickness. The image b shows that the surface of pentacene grains is fully covered by charge injection layer as the self-assembled stacking structure (b) was not seen in Ref. 4. Due to current providing layer with 38 nm of gold, the role at the contact interface only was able to be investigated. S and D stand for source and drain electrodes for OFETs.

25.7–25.8 Ω , Cu: 20.7–21.0 Ω and Al: about 800 Ω , measured values). A 38-nm-thick gold current providing layer was formed on this interlayer to investigate metal dependency at the contact interface only. Scanning electron microscopic images (Magellan, FEI company) of the pentacene surface before and after the deposition of a charge injection interlayer are shown in Figs. 1b and c. The Fig. 1b shows the surface morphology of pentacene, which forms a layer-by-layer structure. Even a metal thin film only 2 nanometer thickness fully covered the step structure on the pentacene surface (Fig. 1c), indicating that the charge injection metal film was sufficiently uniform to study the effect of the contact metal on charge injection. The device fabrication was carried out under both ex-situ (practical) and in-situ (ideal) conditions. The ex-situ fabrication is the more commonly utilized procedure, in which the devices are exposed to an atmosphere before and after thermal evaporation of the source/drain electrodes. On the other hand, the in-situ process was conducted under high vacuum (with $< 10^{-4}$ Pa) and nitrogen (with $\text{H}_2\text{O} < 1$ ppm and $\text{O}_2 < 1$ ppm) for device fabrication, and under nitrogen for the electrical measurements, with no exposure to air. Fabrication and characterization of the devices under these two different sets of conditions were critical for determining the effect of ambient air exposure on the metal/organic interface.

Discussions

The transfer characteristics of OFETs in the saturation region at drain voltage (V_d) = -40 V with three different injection metals obtained under in-situ conditions are presented in Fig. 2a: gold ($W_F = 5.1$ eV), copper ($W_F = 4.65$ eV), and aluminum ($W_F = 4.28$ eV). The largest drain current (I_d) was measured with the order of work functions: gold, copper, and then aluminum. This is because of the difference between the highest occupied molecular orbital (HOMO) of pentacene (about 5.0 eV)⁴ and the Fermi level of the contact metal⁵, based on the work function of contact metals. Furthermore, the charge injection resistances for all samples were obtained through transmission line method (TLM) analysis as contact resistance^{6–9} as shown in

Supplementary Information 1, and were plotted against the work functions. The resulting plot exhibited a linear dependency of contact resistance on work function (Fig. 2b). On the other hand, a significant effect of air exposure was observed in devices fabricated under ex-situ conditions. The electrical characteristics of the same three injection metals showed contrary results to those expected, given the work functions of the metals. The gold interlayer showed the lowest drain current, and the aluminum interlayer showed the best performance despite having the smallest work function (Fig. 2c). In addition, the contact resistances for 11 different charge injection interlayers are plotted in Fig. 2d, and show no dependence on the W_F of the metals. In particular, a beryllium interlayer showed the lowest contact resistance of 1600 Ωcm , which is about a quarter that of metals possessing the largest work function, such as gold or palladium. The reduction of contact resistance enhanced the overall device performance, which results in the improvement of charge injection efficiency. The field effect mobility (μ_{FET}) and threshold voltage for each contact metal were obtained from the transfer character in the saturation region at $V_d = -40$ V, as shown in TABLE I of Supplementary Information 2. Similarly to the reduction of contact resistance, beryllium interlayer indicated 0.69 $\text{cm}^2/\text{V.s}$ for its mobility.

Prior to further investigation, use of TLM plot is concerned under low drain voltage for these devices. Firstly we have shown output characteristics (I_d – V_{sd}) in the linear region under ex-situ and in-situ conditions (Supplementary Information 3). All three contact metals under ex-situ condition show a clear linear relationship under $V_{sd} = -6$ V. A linear relationship indicates the form of ohmic contact at the metal and organic semiconductor interface^{1,10,11}. Notably, the characteristics for copper and aluminum also show the linear relationship although misalignment of energy level between their work functions and HOMO of pentacene is quite large. This implies that an effect of air exposure improves charge injection as well as Fig. 2c. Further, in the case of aluminum whose work function is the smallest of the three metals, the I_d – V_{sd} characteristics show fairly straight line although relatively poor charge injection is expected from its small work function. Another concern is about influence of biasing to contact resistance under large V_{sd} . To investigate this, the transfer characteristics of those three contact metals under both ex-situ and in-situ conditions in the linear region are obtained as shown in Supplementary Information 4. Even low drain voltage condition ($V_d = -1$ V), the characteristics present similar transfer behavior at $V_d = -40$ V in Fig. 2a and 2c. This implies that the device is not much biased. Also, all the TLM plots are evaluated under sufficiently large V_g ($= -40$ V) to avoid that the contact resistance is gate bias-dependent. According to the results from Refs. 12 and 13, when the gate voltage is large enough for efficient charge injection, the change in contact resistances with gate biasing is negligible. Thus, investigation of charge injection through TLM plot in this experiment is feasible.

The comparison of these in-situ and ex-situ in Fig. 2 results suggests a strong influence of air exposure on the metal/organic interface. In particular, the metals which are easily oxidized such as aluminum show the dramatic improvement in charge injection efficiency at the metal/organic contact. One possible interpretation of this improvement is that the natural oxidation of the contact metal probably influences charge injection at the interface to a great extent. To investigate the effect of natural oxide formation at the contact interface, we applied conventional metal oxides, alumina (AlO_x), and silicon oxide (SiO_x), as charge injection interlayers in OFETs. Recently, it is reported that an insertion of thin insulating oxide layer between metal and organic semiconductor improves the charge injection^{14,15}. Here, we also demonstrate that the existence of an oxide at the metal/organic interface can significantly improve charge injection. These insulators can even reduce the contact resistance (Fig. 3). For alumina, the contact resistance was almost the same as with a naturally-oxidized aluminum interlayer. This indicates that contact metal is oxidized easier than chemical reaction with pentacene. Thus,

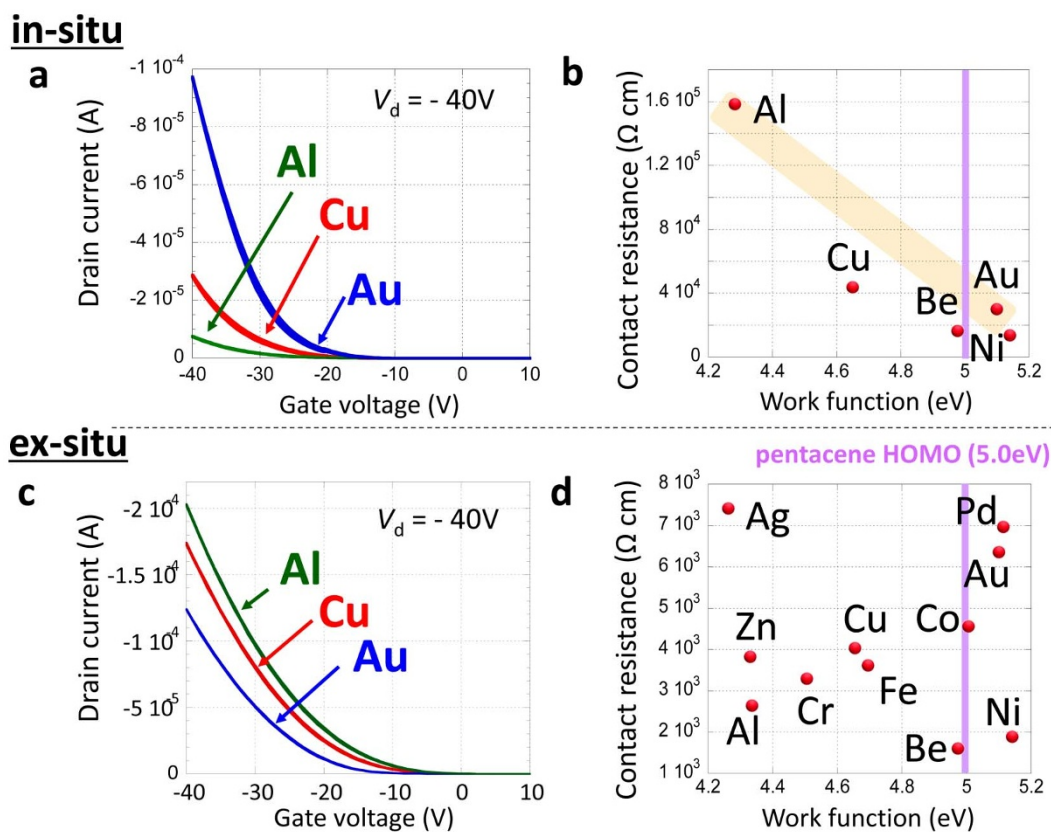


Figure 2 | Plots of (a) transfer characteristics in the saturation region of pentacene OFETs with gold, copper and aluminium charge injection interlayers and (b) contact resistance against work function for 11 different contact metals used as charge injection interlayers. It is noted that the change of shadow mask for metal evaporation and transfer to chamber for electrical characteristic were done under atmosphere, defined as ex-situ condition. Also, plots of (c) transfer characteristics with gold, copper and aluminium, which was processed and characterised under nitrogen and (d) contact resistance against work function for 5 different contact metals under in-situ condition. The bar in orange color in (b) is used for a guide to eyes.

pentacene and contact metal did not make up the chemical composition under ex-situ condition. To support this assumption, Chu *et al.* also reported in Ref. 16 that chemical reaction between the organic layer and the metal electrode by as inserting oxide layers is unfavorable. Additionally, if the devices in Fig. 2a are exposed to an ambient atmosphere after in-situ measurements, the larger current measured follows the same order with ex-situ measurements shown in Fig. 2c, as discussed in Supporting Information 5. This indicates that, under ex-situ conditions, the charge injection interlayer is naturally oxidized, and the resulting oxide layer can reduce the contact resistance. Therefore, the only natural metal oxide is related to the charge injection mechanism.

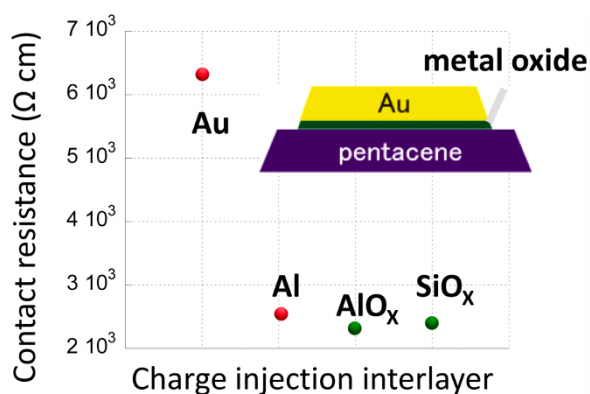


Figure 3 | Contact resistance of each charge injection interlayer (ex-situ condition).

With respect to natural oxidation at the interface, E_p is one possible factor determining charge injection efficiency at the metal/organic semiconductor interface. The electrode potential E_p is the equilibrium potential induced by the electron-transfer process during the reduction-oxidation reaction, and represents a quantitative measure of the tendency of the metal to either loss or gain electrons³. If E_p of the metal is low, the metal tends to be oxidized easily. The E_p is similar in concept to the W_F , since both indicate potentials for electron transfer processes. However, the two have entirely different tendencies (Fig. 4a). The work function represents the energy required to remove an electron to the vacuum level (ideal condition: in this experiment under in-situ condition) from the Fermi level of the metal, but E_p represents the potential required to lose or gain electrons via reduction or oxidation process (practical condition: under ex-situ condition).

The Fig. 2c, the contact resistances of 11 different contact metals under ex-situ conditions, was re-plotted against E_p (Fig. 5a). As the contact metal E_p decreased, the contact resistance was also reduced, in a linear relationship. On the other hand, under in-situ conditions, E_p showed no correlation with the contact resistance, as shown in Fig. 5b. Therefore, negative values of the standard electrode potential, which implies natural oxidation occurs easily, is another important factor in the determination of charge injection efficiency at the metal/organic contact interface after air exposure. Furthermore, a correlation between the contact resistance and E_p becomes more obvious in interface metals with similar work functions, such as the green ($W_F = 4.26$ to 4.33 eV) and pink regions ($W_F = 4.95$ to 5.15 eV) in Fig. 4a. As seen in Figs. 4b and c, a linear relationship was exhibited. Also, it should be noted that the contact resistances of 11 different charge injection interlayers are plotted with other possible physical factors: electronegativity, electron affinity and ionization energy (1st)

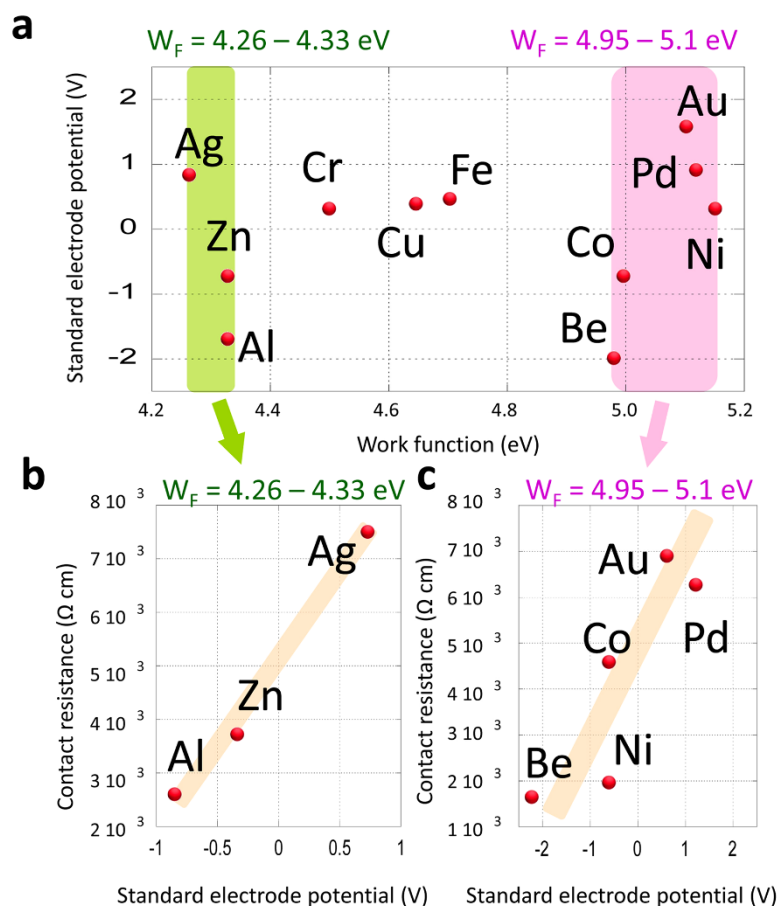


Figure 4 | (a) A plot of standard electrode potential against work function of 11 contact metals used. The bars in green region within 4.26–4.33 eV of work function and in pink region within 4.95–5.15 eV. In the two regions the contact resistances are plotted against standard electrode potential respectively (b and c). The bars in orange color are used for a guide to eyes.

as shown in Supplemental Information 6. It seems that electronegativity would have some tendency with linear relationship. However, electronegativity is defined as a chemical property to describe how much energy is required to attract an electron toward the atom in vacuum. It means that this factor cannot describe the improvement of charge injection after air exposure. Thus, those factors do not show any clear correlation with contact resistance, with the comparison of the case for standard electrode potential in Fig. 5a. From these analyses we concluded that standard electrode potential is possible or the

most likely factor to show the correlation with charge injection efficiency on the practical interface. The metal/organic interface properties are clearly influenced by natural oxidation of the contact metal, according to the above correlation with E_p . The naturally oxidized contact metal forms variable states around the original valence band (V.B.) and conduction band (C.B.) at the interface between the current providing layer and pentacene. The density of states near the V.B. and C.B. may be widely distributed, because natural oxides generally form a non-crystalline amorphous phase with a mixture

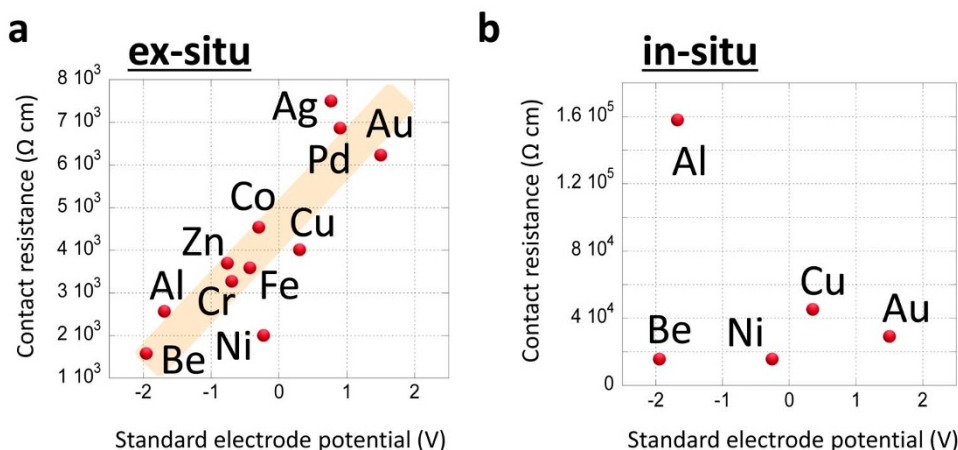


Figure 5 | Plots of contact resistance against standard electrode potentials obtained in Fig. 2(a) under ex-situ condition (a) and under in-situ condition (b). The bar in orange color in (a) is used for a guide to eyes.

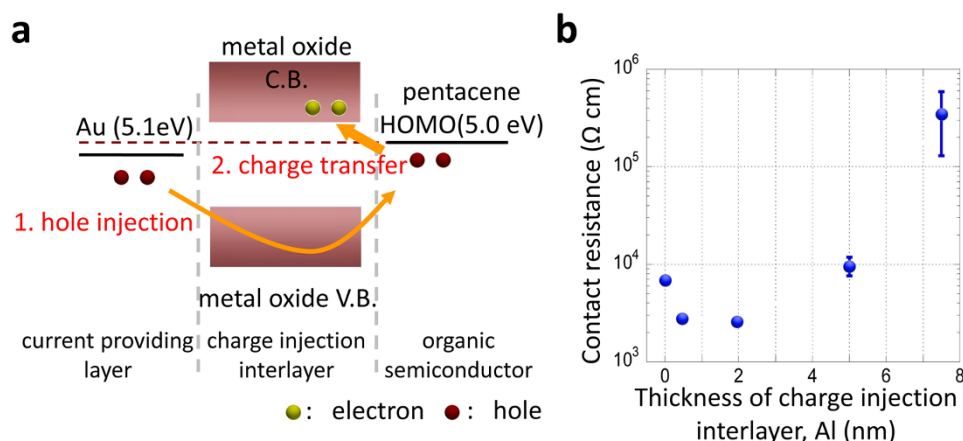


Figure 6 | (a) A schematic of two possible charge injection mechanisms induced by naturally oxidised contact metal: 1. Charge injection from the Fermi level of gold to the HOMO of pentacene via the V.B. of natural metal oxide and 2. Charge transfer from HOMO of pentacene to C.B. of natural metal oxide. The dashed line in red colour is a guide to eyes. The presented C.B. and V.B. bands show as wide gray bar because they consist of a few series of oxide bands such as natural aluminium oxide forms diffused V.B. and C.B. due to amorphous structure of natural oxide^{27–33}. (b) A plot of thickness dependent for aluminium charge injection interlayer against contact resistance.

of oxide structures. Two possible mechanisms can be considered for charge injection at this interface. One is a charge injection process through the V.B. of the natural metal oxide into the HOMO of pentacene (mechanism 1 in Fig. 6a), and the other is charge transfer between the HOMO of pentacene and the C.B. of the oxide (mechanism 2 in Fig. 6a). The former mechanism helps smooth charge injection from the current providing layer into the organic semiconductor through the V.B. of the oxide film. This was reported by number of researchers^{16–21}, in order to reduce the misalignment of energy levels between the Fermi level of the metal and the HOMO of the organic semiconductor. The other mechanism is electron transfer from the HOMO of pentacene to the C.B. of the natural metal oxide. This charge transfer creates holes at the interface, similar mechanism is described in the Ref. 21. Consequently, it reduces the trap states in the vicinity of the contact as the doping effect^{22–24}. Interface dipole is also considerable at the metal/organic semiconductor interface confined to a narrow interlayer^{25,26}. In the experimental results of Refs. 14 and 15 and our results in Fig. 3, even insulating oxides such as aluminum oxide and silicon dioxide improved the charge injection. Those insulating oxide layers would not facilitate interface dipole. Similarly, the tunneling effect could be applied to the mechanism with the thin interlayer. In the case of tunneling effect, the thin metal oxide layer acts as potential barrier. This means that during transport, a portion of carriers is scattered by the potential barrier. Also, the improvement of current with constant voltage applied to the device cannot be explained by the tunneling effects. To support this mechanism, the contact resistance for silver shows a poor charge injection as shown in Fig. 2(d). If tunneling effect is applicable here, contact metal with low work function such as silver cannot provide improved charge injection efficiency although aluminum whose work function is close to silver improved the charge injection as shown in Fig. 2(d). Therefore, the charge transfer process induces more efficient charge injection at the metal and organic semiconductor interface. The thickness dependency of the aluminum charge injection interlayer is shown in Fig. 6b. An improvement of charge injection was demonstrated, even when the injection layer was as thin as 0.5 nm. However, if the interlayer is too thick, metals such as aluminum, which produce an insulating oxide film^{27–33}, are ineffective because the metal oxide prevents charge injection. However, metals which do not produce an insulator through natural oxidation, such as copper, are not influenced by the thickness of the interlayer, as described in Refs. 34 and 35.

In conclusion, based upon systematic experiments, we propose that natural oxidation of the contact metal strongly influences charge

injection through the metal/organic semiconductor interface. After exposure to ambient air, the standard electrode potential of the metal can be the most important factor governing charge injection and determining the contact resistance of organic devices. The spontaneous formation of an oxide film at the contact may cause effective charge injection through states near the V.B. of the oxide film, or may act as a dopant due to charge transfer from the organic semiconductor. Understanding these mechanisms is very useful for contact interface engineering, which can dramatically improve the charge injection efficiency in any organic device. This is because the present results was performed for practical experimental condition while ideal discussion was based on the W_F -values observed on the ultra-clean surface in very high vacuum condition.

Methods

Device fabrications and characterization. Highly doped $p+$ silicon wafers with a 200-nm-thick layer of thermal oxide were employed as substrates. The substrates were coated with beta-phenethyltrichlorosilane (Sigma-Aldrich, 95%) as a self-assembling monolayer, following the recipe given in Ref. 36. Pentacene (Sigma-Aldrich, twice-purified using temperature gradient sublimation) was thermally evaporated to a 40-nm thickness at a rate of 0.1 Å s^{-1} . For the ex-situ case, the substrates were exposed to an ambient atmosphere while shadow masks were exchanged to define the double-layer OFET electrodes. The charge injection interlayer (various metals, 2 nm thick) was thermally evaporated at 0.2 Å s^{-1} , and the current providing layer (Au, 38 nm thick) was then deposited at the same rate. After fabrication, seven OFETs were defined with the same channel width of 750 μm , and various channel lengths of 20–140 μm with an interval of 20 μm , as shown in Supplementary Information 1. The samples were transferred into a high vacuum chamber ($< 10^{-4} \text{ Pa}$) for transistor characterization (Agilent 4165A and C). Note that this transfer process was also performed under exposure to ambient atmosphere. For the in-situ case, all procedures including the exchange of shadow masks and measurement of electrical characteristics were carried out under nitrogen with H_2O and O_2 concentrations below 1 ppm and no air exposure. The other thermal evaporation parameters were similar to those used in the ex-situ case.

1. Sze, S. M. & Ng, K. K. *Physics of Semiconductor Devices* (Wiley, New York, 1981).
2. Ishii, H. *et al.* Energy Level Alignment and Interfacial Electronic Structures at Organic/Metal and Organic/Organic Interfaces. *Adv. Mater.* **11**, 605 (1999).
3. Bard, A. J. *et al.* *Standard Potential in Aqueous Solutions* (Marcel Dekker, Inc., New York, 1985).
4. Ozaki, H. Growth of organic ultrathin films studied by Penning ionization electron and ultraviolet photoelectron spectroscopies: Pentacene. *J. Chem. Phys.* **113**, 6361 (2000).
5. Michelson, H. B. The work function of the elements and its periodicity. *J. Appl. Phys.* **48**, 4729 (1977).
6. Kluak, H. *et al.* Contact resistance in organic field effect transistors. *Solid-State Electron* **47**, 297 (2003).
7. Pesavento, P. V. *et al.* Gated four-probe measurements on pentacene thin-film transistors: Contact resistance as a function of gate voltage and temperature. *J. Appl. Phys.* **96**, 7312 (2004).



8. Necliudov, P. V. *et al.* Modeling of organic thin film transistors of different designs. *J. Appl. Phys.* **88**, 6594 (2000).
9. Tiwari, S. P. *et al.* Pentacene organic field-effect transistors with doped electrode-semiconductor contacts. *Org. Electron.* **11**, 860 (2010).
10. Klauk, H. *Organic Electronics: Materials, Manufacturing, and Applications* (Wiley-VCH: Weinheim, Germany, 2006).
11. Bao, Z. & Locklin, J. *Organic Field-Effect Transistors* (CRC Press, 2007).
12. Vinciguerra, V. *et al.* Modeling the gate bias dependence of contact resistance in staggered polycrystalline organic thin film transistors. *Org. Electron.* **10**, 1074 (2009).
13. Reese, C. & Bao, Z. Detailed Characterization of Contact Resistance, Gate-Bias-Dependent Field-Effect Mobility, and Short-Channel Effects with Microscale Elastomeric Single-Crystal Field-Effect Transistors. *Adv. Funct. Mater.* **19**, 763 (2009).
14. Darmawan, P. *et al.* Reduction of charge injection barrier by 1-nm contact oxide interlayer in organic field effect transistors. *Appl. Phys. Lett.* **100**, 013303 (2012).
15. Kim, H. *et al.* Improvement of the contact resistance between ITO and pentacene using various metal-oxide interlayers. *Org. Electron.* **9**, 1140 (2008).
16. Chu, C.-W. *et al.* High-performance organic thin-film transistors with metal oxide/metal bilayer electrode. *Appl. Phys. Lett.* **87**, 193508 (2005).
17. Matsushima, T. *et al.* Formation of Ohmic hole injection by inserting an ultrathin layer of molybdenum trioxide between indium tin oxide and organic hole-transporting layers. *Appl. Phys. Lett.* **91**, 253504 (2007).
18. Meyer, J. *et al.* Effect of contamination on the electronic structure and hole-injection properties of MoO₃/organic semiconductor interfaces. *Appl. Phys. Lett.* **96**, 133308 (2010).
19. Kim, D. Y. *et al.* The effect of molybdenum oxide interlayer on organic photovoltaic cells. *Appl. Phys. Lett.* **95**, 093304 (2009).
20. Kano, M. *et al.* Improvement of subthreshold current transport by contact interface modification in p-type organic field-effect transistors. *Appl. Phys. Lett.* **94**, 143304 (2009).
21. Kröger, M. *et al.* Role of the deep-lying electronic states of MoO₃ in the enhancement of hole-injection in organic thin film. *Appl. Phys. Lett.* **95**, 123301 (2009).
22. Schroeder, R. *et al.* Improving organic transistor performance with Schottky contacts. *Appl. Phys. Lett.* **84**, 1004 (2002).
23. Minari, T. *et al.* Charge injection process in organic field-effect transistors. *Appl. Phys. Lett.* **91**, 053508 (2009).
24. Minari, T. *et al.* Highly enhanced charge injection in thienoacene-based organic field-effect transistors with chemically doped contact. *Appl. Phys. Lett.* **100**, 093303 (2012).
25. Hamadani, B. H. *et al.* Doping-dependent charge injection and band alignment in organic field-effect transistors. *Phys. Rev. B* **72**, 235302 (2005).
26. Knupfer, B. H. & Paasch, G. Origin of the interface dipole at interfaces between undoped organic semiconductors and metals. *J. Vac. Sci. Technol. A* **23**, 1072 (2005).
27. Cowan, J. J. & Arakawa, E. T. Dispersion of surface plasmons in dielectric-metal coatings on concave diffraction gratings. *Z. Phys.* **235**, 97 (1970).
28. Pettit, R. B. *et al.* Measurement of surface-plasmon dispersion in oxidized aluminum films. *Phys. Rev. B* **11**, 3116 (1975).
29. Watts, J. F. & Wolstenholme, J. *An Introduction to Surface Analysis by XPS and AES* (Marcel Dekker, Inc., New York, 1985).
30. Kang, H. *et al.* High mobility, low voltage polymer transistor. *Org. Electron.* **8**, 460 (2007).
31. Miyazaki, H. *et al.* *Semicond. Sci. Technol.* **25**, 034008 (2010).
32. Desai, S. R. *et al.* A study of the structure and bonding of small aluminum oxide clusters by photoelectron spectroscopy: Al_xO_y (x51–2, y51–5). *J. Phys. Chem.* **106**, 1309 (1997).
33. Gautier, M. *et al.* Modifications of α -Al₂O₃ (0001) surfaces induced by thermal treatments or ion bombardment. *Surf. Sci.* **250**, 71 (1991).
34. Wang, S. D. *et al.* Contact-metal dependent current injection in pentacene thin-film transistors. *Appl. Phys. Lett.* **91**, 20358 (2007).
35. Lu, X. *et al.* Effect of air exposure on metal/organic interface in organic field-effect transistors. *Appl. Phys. Lett.* **98**, 243301 (2011).
36. Kumaki, D. *et al.* Air stable, high performance pentacene thin-film transistor fabricated on SiO₂ gate insulator treated with β -phenethyltrichlorosilane. *Appl. Phys. Lett.* **90**, 133511 (2007).

Acknowledgements

Authors greatly acknowledge to Dr. Miyazaki, Dr. Liu and Dr. Lu (National Institute for Materials Science, Japan) and Dr. James Stott (London Centre for Nanotechnology, United Kingdom) for fruitful discussions and to Dr. Murata in FEI company for SEM images.

Authors Contributions

A.K. performed all the experiments and wrote the manuscript. A.K., T.M. and K.T. planned, and all the authors analysed the experimental results.

Additional information

Supplementary information accompanies this paper at <http://www.nature.com/scientificreports>

Competing financial interests: The authors declare no competing financial interests.

License: This work is licensed under a Creative Commons Attribution-NonCommercial-ShareAlike 3.0 Unported License. To view a copy of this license, visit <http://creativecommons.org/licenses/by-nc-sa/3.0/>

How to cite this article: Kumatani, A., Li, Y., Darmawan, P., Minari, T. & Tsukagoshi, K. On Practical Charge Injection at the Metal/Organic Semiconductor Interface. *Sci. Rep.* **3**, 1026; DOI:10.1038/srep01026 (2013).